
EFFECT OF NIOBIUM ADDITION ON THE ELECTROCHEMICAL AND MECHANICAL PROPERTIES OF TITANIUM ALLOYS AS BIOMATERIALS

By

Adam Arlei Dipodiwiryo¹, Djoko Hadi Prajitno², Raden Dadan Ramdan³, Riza Wirawan⁴

^{1,3,4}Department of Materials Engineering, Bandung Institute of Technology

²Badan Riset dan Inovasi Nasional

E-mail: ¹dipodiwiryo@gmail.com, ²djok00@brin.go.id, ³dadan@material.itb.ac.id,

⁴riza.wirawan@itb.ac.id

Article History:

Received: 10-08-2024

Revised: 19-08-2024

Accepted: 27-09-2024

Keywords:

Titanium Alloy, Electric Arc Furnace, Corrosion Resistance, Mechanical Properties

Abstract: Titanium is a metal known for its high strength, lightweight, and excellent corrosion resistance, making it widely used as a biomaterial in medical applications. To further enhance these properties, particularly corrosion resistance and mechanical strength, niobium (Nb) was added to titanium-aluminum (Ti-Al) alloys. In this study, three alloy compositions, Ti-5Al-10Nb, Ti-5Al-8Nb, and Ti-5Al-6Nb, were fabricated using the Electric Arc Furnace (EAF) method. After the melting process, the specimens were characterized using Scanning Electron Microscopy (SEM) combined with Energy Dispersive Spectroscopy (EDS) to analyze the microstructure and alloying element distribution. X-Ray Diffraction (XRD) was employed to identify the crystalline phases formed in the alloys. Electrochemical testing was performed using the Tafel polarization method to measure corrosion rates, while mechanical testing was conducted using the Vickers hardness test to determine material hardness. The results showed that increasing niobium content in the titanium alloy significantly improved the corrosion resistance and hardness of the specimens. The Ti-5Al-10Nb specimen exhibited the lowest corrosion rate and highest hardness compared to the other specimens. These findings suggest that the addition of niobium can enhance the performance of titanium alloys as biomaterials, particularly for hip joint implant applications.

INTRODUCTION

Biomaterials are a rapidly advancing technology in the medical field, used to replace the function of damaged organs or tissues. In their development, biomaterials are required not only to have adequate mechanical properties but also biocompatibility, which refers to

the ability of the material to interact with body tissues without causing significant rejection reactions (Bogdan and Bogdan 2021). The human body has a complex defense mechanism against foreign objects, so biomaterials must be able to adapt to these conditions without triggering adverse immunological responses. Factors such as chemical composition, surface properties, and degradation rate greatly influence the biocompatibility of a material.

Titanium and its alloys have become one of the primary materials of choice as biomaterials due to their high strength, low density, and good biocompatibility. The Ti-6Al-4V alloy, for example, has been widely used because of its superior mechanical properties. However, long-term use of this alloy raises concerns regarding the potential release of vanadium and aluminum, which are known to be toxic to the human body (Y, C and H 2014). As a result, research has focused on the development of new titanium alloys that do not contain vanadium, such as Ti-6Al-7Nb, where vanadium is replaced by niobium (Nb).

The melting of titanium alloys involves methods capable of reaching very high temperatures to melt elements such as titanium, aluminum, and niobium, which have melting points of 1,668°C, 660°C, and 2,476°C, respectively (National Library of Medicine 2023). One effective method is the Electric Arc Furnace (EAF), which uses an electric arc to achieve high melting temperatures (Omazaki 2023). The EAF can heat materials up to 3,500°C, and argon gas is often used to prevent oxidation during the melting process (A, et al. 2019).

In medical applications, corrosion resistance is a key factor in the selection of biomaterials. The human body is a highly corrosive environment due to interactions with body fluids (Reddi 2023). Corrosion testing is often conducted using a three-electrode potentiostat method, where the working electrode is the specimen being tested, the reference electrode is used to control the potential, and the counter electrode is an inert metal such as platinum (Iuri, et al. 2008). The testing medium is usually an infusion fluid solution that simulates conditions within the human body (Reddi 2023).

Currently, research on the effect of niobium on titanium alloys, especially with niobium content below 10%, is still limited. This study aims to explore the effect of varying niobium compositions on the electrochemical and mechanical properties of Ti-Al-Nb alloys. The alloys are fabricated using the Electric Arc Furnace (EAF) method, with the hope that the results will provide new insights into optimizing niobium composition in titanium alloys as biomaterials.

LITERATURE REVIEW

Titanium and its alloys are widely used as biomaterials due to their high strength, lightweight, and good corrosion resistance. At room temperature, pure titanium is generally in the alpha (α) phase, which has a hexagonal close-packed (HCP) structure and offers better corrosion resistance compared to the beta (β) phase, which has a body-centered cubic (BCC) structure (R 2010). These twophase equilibrium regions are separated by the transus temperature point (882°C). The addition of niobium (Nb) as a beta-stabilizing element can be used to stabilize the beta phase at temperatures below the transus point, even down to room temperature. The beta phase stabilized by Nb exhibits better corrosion resistance compared to pure alpha phase.

METHODOLOGY

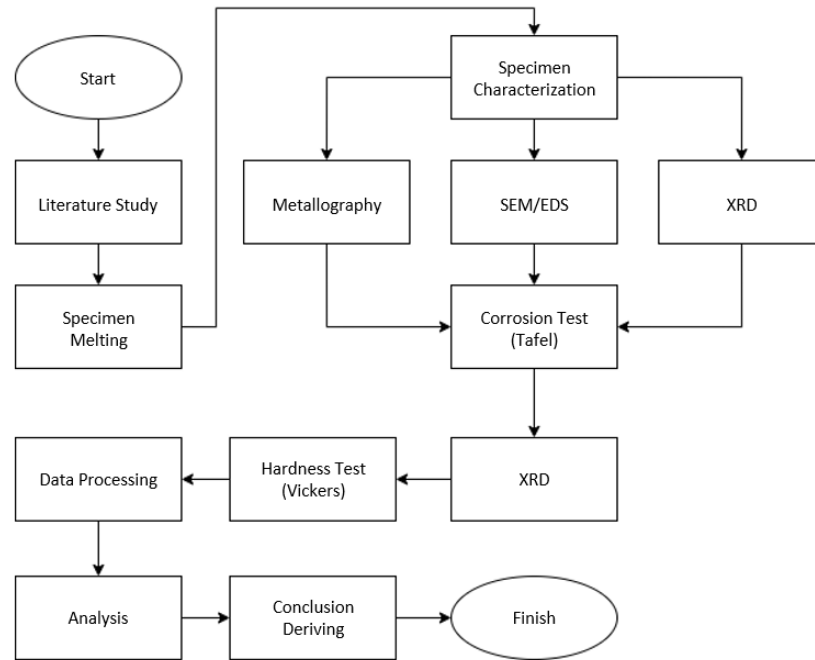


Figure 1. Research Flowchart

This research uses three variations of titanium-niobium-aluminum alloys, namely Ti-5Al-10Nb (A), Ti-5Al-8Nb (B), and Ti-5Al-6Nb (C). The materials used in this study include pure titanium plates, pure aluminum pellets, pure niobium wires, Ringer Lactate solution, platinum rods, and Ag/AgCl. The equipment used includes an analytical balance for measuring the materials, an Electric Arc Furnace (EAF), SEM (Scanning Electron Microscope)/EDS (Energy Dispersive Spectroscopy), XRD (X-Ray Diffraction), a three-electrode potentiostat, and a Vickers hardness tester.

The research process began with the alloy fabrication. The titanium, aluminum, and niobium were weighed according to the design, then melted using the EAF. The melting process was conducted in an argon gas atmosphere to prevent oxidation of the alloy. After the melting process was complete, the specimens were cut and modified to fit the testing standards. The next step involved specimen characterization, which included microstructure observation following ASTM E3 standards (ASTM 2017) and elemental composition analysis using SEM/EDS following ASTM E1508-12a standards (ASTM 2019). In addition, XRD was used to analyze the crystalline phases formed in the alloy. XRD was performed both before and after the corrosion test. Following characterization, the specimens were tested for their electrochemical and mechanical properties.

The corrosion resistance of the specimens was tested using the Tafel polarization method with a three-electrode potentiostat. The cut specimen was placed as the working electrode (WE), while the reference electrode (RE) used was Ag|AgCl, and the counter electrode (CE) was platinum. The electrolyte solution used was Ringer Lactate, simulating human body fluids. The testing was conducted following ASTM G5 standards (ASTM 2021). The test results were expressed in corrosion rates (mils per year).

The hardness test was conducted using the Vickers hardness test. Each specimen was mounted in epoxy resin and tested using a diamond indenter shaped like a pyramid with a 136° angle and a load of 2 kgf. The testing was conducted based on ASTM standards (ASTM 2023). The Vickers hardness value was calculated based on the average indentation produced and expressed in HV (Vickers Hardness).

RESULTS AND DISCUSSION

Material Characterization

In this research, the SEM/EDS machine was used to check for the presence of elements in the alloy. Using a voltage parameter of 5.00 kV, elemental readings were taken using the area method for the three specimens, as shown in Figure 2.

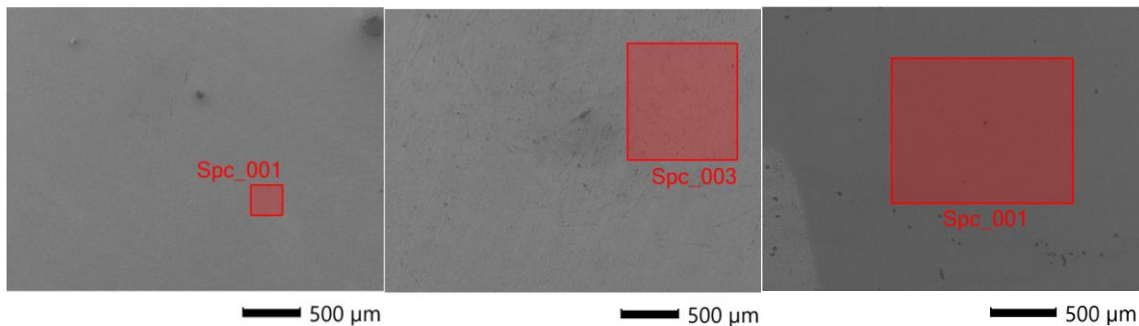


Figure 2. EDS reading area on specimen A (left), B (middle), C (right)

From the readings, the EDS spectrum, which is an energy-intensity curve, was obtained as shown in Figure 3. The spectrum was then compared with a database containing EDS spectra of all previously identified elements, allowing for matching.

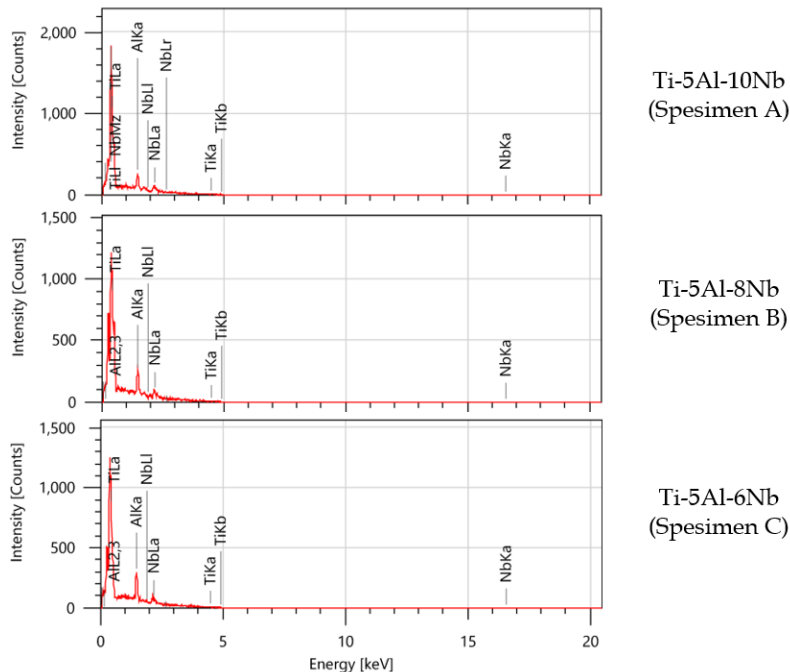


Figure 3. EDS spectrum for the three alloy specimens

The matching results performed by the computer indicate that titanium, aluminum, and niobium were detected in the spectrum above. The intensity of each detected element can then be quantified into relative weight percentages. The weight percentage of elements for each specimen from one reading can be seen in Table 1.

Table 1. The percentage of elements detected by EDS

Elements	Specimen [wt%]		
	A	B	C
Ti	89,62	85,19	87,12
Al	3,04	5,44	5,61
Nb	7,34	9,36	7,27

The elemental weight percentages detected by EDS in Table 1 differ from the alloy design before melting. Specimen A shows the most significant difference from its initial design, with the aluminum percentage expected to be 5% but found to be only 3.04%. Additionally, the niobium percentage in specimen A, which should be 10%, was detected as only 7.34%. Similarly, specimens B and C also showed differences in elemental percentages in this reading. This could be due to element distribution inhomogeneity in the specimen, as checking other points on specimen A revealed that the alloy element fractions also changed. The aluminum fraction increased to 6.64% and niobium to 10.96%.

Metallography

The first observation made on the melted Ti-Al-Nb alloys was metallography. Figure 4 shows the typical microstructure of the three specimens. In the image, it can be observed that specimen A (Ti-5Al-10Nb) and specimen B (Ti-5Al-8Nb) form equiaxial (1 and 2) and dendritic (4 and 5) microstructures. Meanwhile, specimen C (Ti-5Al-6Nb) forms Widmanstätten (3) and basket-weave (6) microstructures.

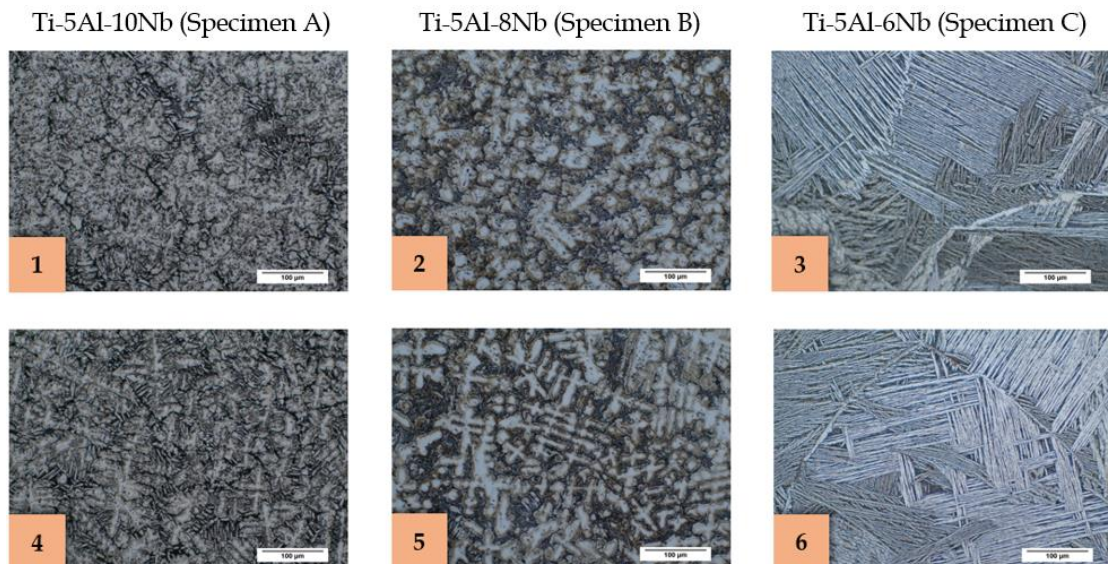


Figure 4. The microstructure of each specimen

The differences in microstructure among specimens A, B, and C may be due to the amount of Nb contained. Niobium, as an element that acts as a β -stabilizer, expands the β phase equilibrium region. This results in more β phase being retained during cooling in specimens with higher niobium composition. In Figure 4, the α phase is indicated by white/bright areas, and the β phase is indicated by black/dark areas. The phase fractions of the alloy can be represented by the phase area fractions since the specimens are isotropic. All microstructure images of each specimen were processed using the threshold function in the ImageJ application to obtain phase area fraction values. Figure 5 presents the phase fractions of the three specimens in the form of a bar chart. It was found that the β phase area fraction in the titanium alloy increases with higher niobium concentration. This is consistent with the hypothesis based on the Ti-Nb phase diagram, which indicates that more niobium leads to a higher β phase content in the specimen due to the formation of a β phase solid solution with niobium.

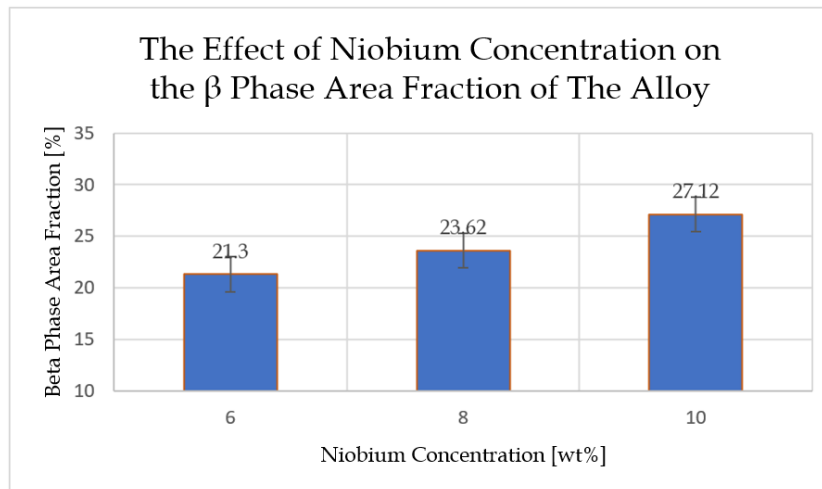


Figure 5. The β phase area fraction for each niobium concentration

In addition to differences in phase composition, variations in composition also lead to differences in the morphology of the obtained microstructures. These morphological differences could be due to variations in thermal conductivity at different positions within the alloy. The three elements forming the alloy in this study have different thermal conductivity values: 210.0 W/mK for aluminum (Al), 52.3 W/mK for niobium (Nb), and 17.0 W/mK for titanium (Ti) (Matweb n.d.). Areas with higher concentrations of alloying elements result in more random thermal conductivity distributions. This leads to a more irregular solidification process, resulting in dendritic structures.

Observations using SEM/EDS reveal the elemental composition of each specimen of Ti-5Al-10Nb, Ti-5Al-8Nb, and Ti-5Al-6Nb alloys. EDS analysis results show variations in the detected elemental composition, with some differences from the intended composition due to inhomogeneities during the melting process. The detected elemental percentages in specimen A are 89.62% titanium, 3.04% aluminum, and 7.34% niobium. Specimens B and C also show similar variations with differences in the resulting elemental contents.

XRD (X-Ray Diffraction)

XRD characterization was performed to obtain spectra of the phases present in the specimens before and after electrochemical testing. By analyzing the XRD graphs from both conditions of the specimens, changes in the quantity of phases present can be observed. Figure 6 presents the XRD graphs of specimen B (Ti-5Al-8Nb) before and after the Tafel test.

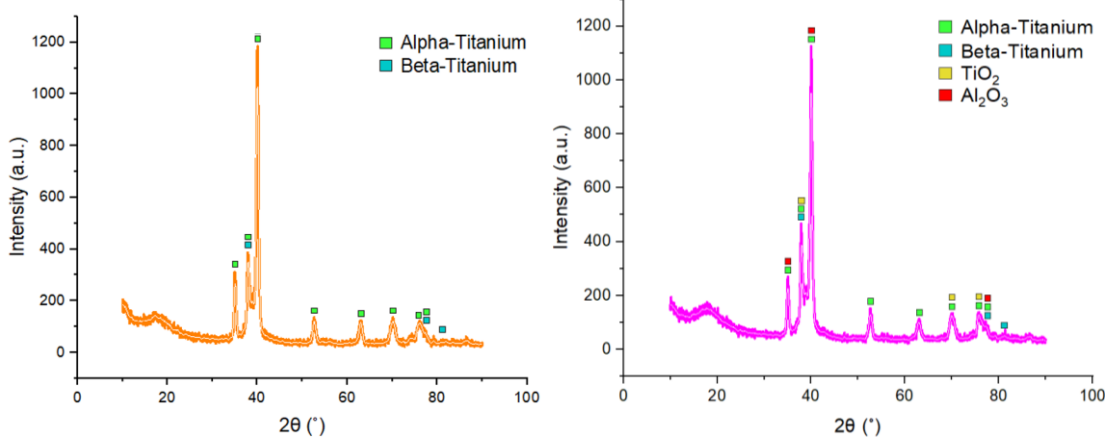


Figure 6. XRD graphs of specimen B (Ti-5Al-8Nb) before (left) and after (right) electrochemical testing

The two graphs, after being processed with the X'Pert Highscore Plus application using the JCPDS database, show the presence of α -titanium (00-001-1198), β -titanium (01-088-2321), TiO_2 (00-001-0562), and Al_2O_3 (00-001-1307). When both graphs are plotted on the same diagram, differences in the intensity of phases or oxides in the two conditions of the specimens can be observed. Figure 7 shows a diagram that is a compilation of the two graphs from Figure 6, with the 2θ values of the specimen before the Tafel test shifted by 1 degree to prevent overlapping peaks.

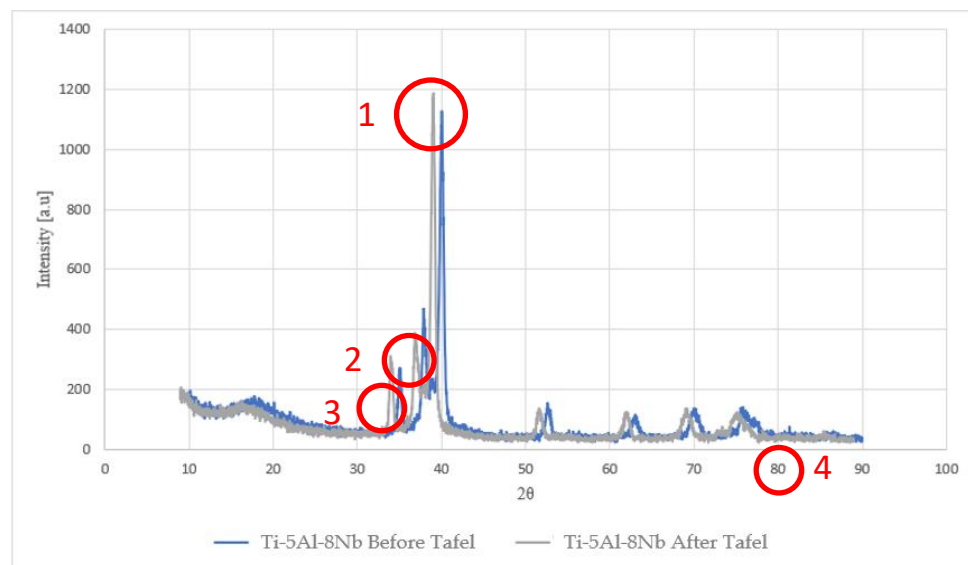


Figure 7. Differences in the XRD graphs of Ti-5Al-8Nb before and after the Tafel test

The peaks that decrease after the Tafel test at red circles '1' and '3' indicate a reduction in the percentage of α -titanium. The red circle '2' shows the formation of TiO_2 . The red circle '4' indicates the formation of Al_2O_3 in the specimen. This explains the phenomena observed during the Tafel test, namely the formation of TiO_2 from α -titanium and the sacrificial behavior of aluminum to form Al_2O_3 , due to its greater affinity for oxygen compared to titanium.

Corrosion Test (Tafel)

Electrochemical testing was conducted using a three-electrode potentiostat with a reference electrode (RE) of $Ag|AgCl$ in KCl and a counter electrode (CE) of platinum, in an electrolyte medium of Ringer Lactate at a temperature of $25^\circ C$.

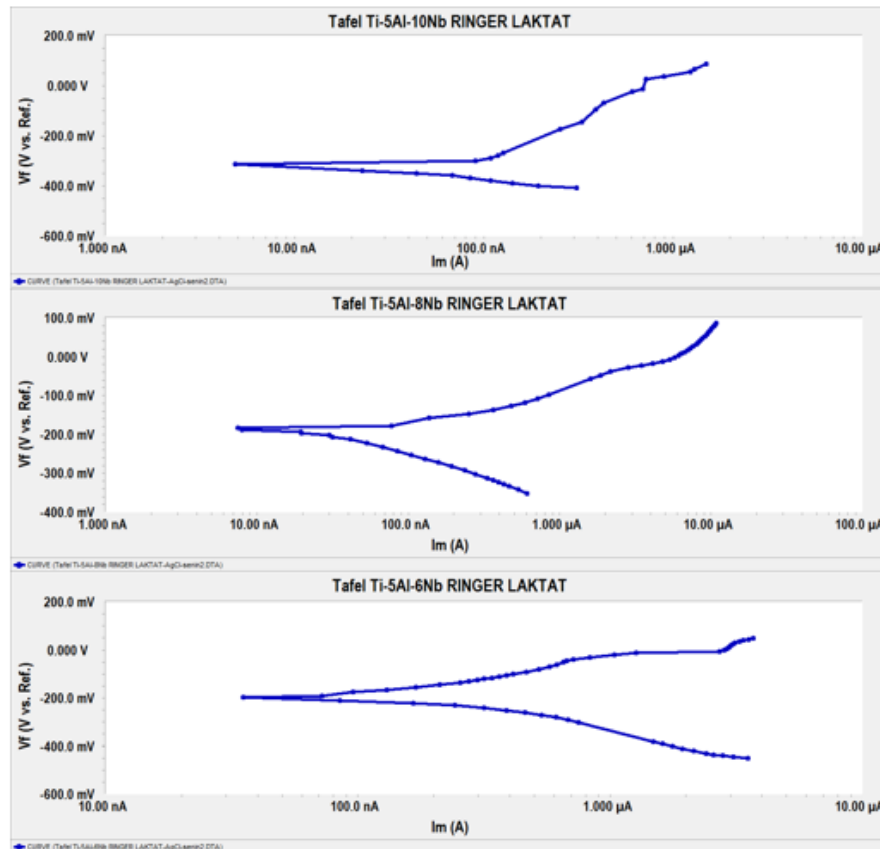


Figure 8. Tafel polarization curves of the three alloy specimens

The data obtained from the potentiostat testing is presented as current versus potential curves, as shown in Figure 8. Using the Tafel fitting function in the Gamry Echem Analyst application, the analysis of these graphs produces data on corrosion rates. This calculation is based on Faraday's law, which is then modified into the following formula:

$$CR = K \frac{icorr}{\rho A} EW$$

In the formula, CR is the corrosion rate with units of depth of corrosion per time. K is

a constant with a value of 1.288×10^{-1} mils/(A cm year). Icorr is the corrosion current in amperes, ρ is the density of the alloy, A is the surface area of the specimen in cm^2 , and EW is the equivalent weight in grams. The results of the corrosion rate calculations for each specimen are then plotted as a bar chart, as shown in Figure 9.

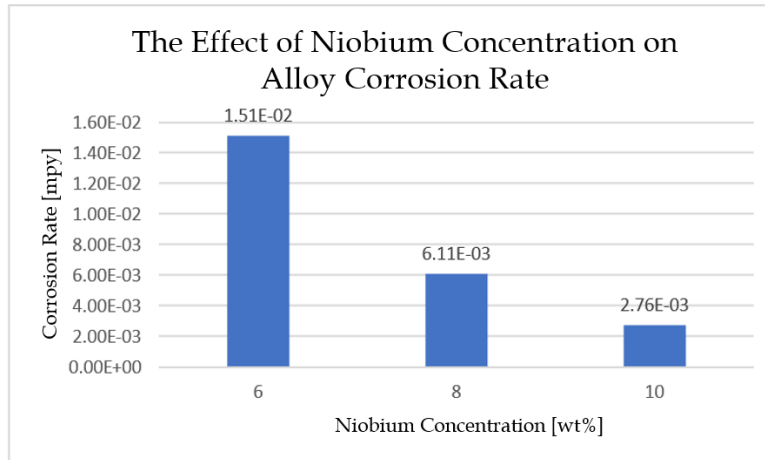


Figure 9. Niobium concentration values versus the corrosion rate of the alloy

The corrosion rate of each specimen shows results consistent with the hypothesis that higher niobium concentration leads to a lower corrosion rate in a titanium alloy. Niobium can enhance the corrosion resistance of the titanium alloy by stabilizing the β phase through the formation of a solid solution. This phase has higher biocorrosion resistance compared to the α phase (Mohammed, Khan and Siddiquee 2014).

Hardness Test (Vickers)

Vickers hardness testing was performed with a load parameter of 2 kgf and a diamond pyramid indenter with a 136° angle on all three alloy specimens. Indentations were made six times at different points on each specimen to obtain a sufficient dataset. The resulting hardness values were then plotted as a bar chart, as shown in Figure 10.

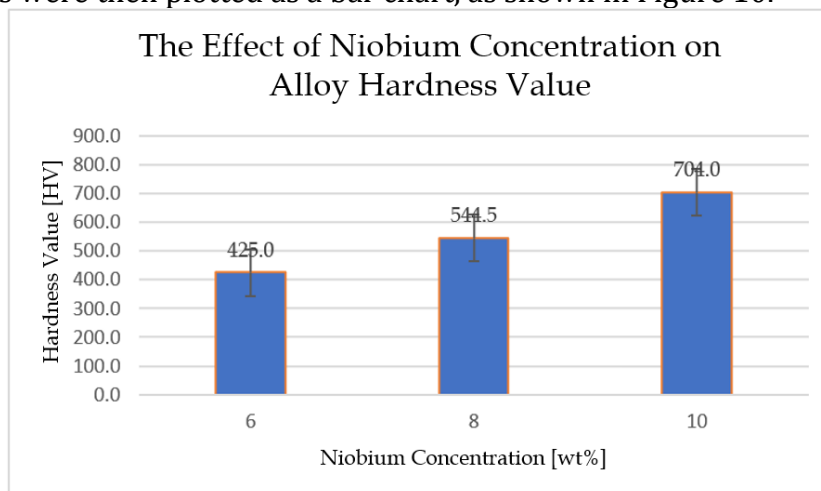


Figure 10. Niobium concentration values versus the average hardness of the specimens

It was found that the average hardness value of the specimens increases with the concentration of niobium. In pure titanium, the β phase, which has a BCC configuration, should have a lower atomic packing factor compared to the α phase with an HCP configuration, and therefore a lower hardness value than the α phase. Thus, an increase in the β phase fraction would make titanium softer. However, in this case, according to Hume-Rothery rules, Ti and Nb form a substitutional solid solution because the atomic radius difference between the two elements is less than 15%. The presence of substitutional atoms causes distortion in both α and β lattices, which can impede dislocation movement. This makes the material more resistant to plastic deformation, thus increasing its hardness value.

CONCLUSIONS

This research successfully fabricated titanium-aluminum-niobium alloys using the electric arc melting (EAF) method with compositions of Ti-5Al-10Nb, Ti-5Al-8Nb, and Ti-5Al-6Nb. Although this melting process demonstrated good results in alloy formation, some inhomogeneities in element distribution were observed, which may affect the final properties of the material. This indicates the need for improvements in the fabrication process to ensure better material homogeneity in the future.

Electrochemical testing using the Tafel method showed that increasing the niobium content in the alloy significantly improves corrosion resistance. This finding confirms the role of niobium as a beta-stabilizer that strengthens the beta phase and forms a more effective passive oxide layer, thereby reducing the corrosion rate in an environment simulating body conditions. Additionally, Vickers hardness test results indicate that niobium addition also enhances the alloy's hardness. The distortion in the crystal structure due to niobium substitution leads to increased resistance to plastic deformation, providing better mechanical properties to the alloy.

As a recommendation, annealing techniques after melting are suggested to achieve better alloy homogenization and ensure more uniform element distribution. Corrosion testing could be expanded using more complex electrolyte solutions that more closely resemble human body fluids. Furthermore, the use of EDS Mapping or OES methods is recommended for further validation regarding element distribution in the alloy, which could provide a more accurate understanding of material homogeneity.

REFERENCES

- [1] A, Paganotti, Bessa C.V.X., Silva L.S., and Silva R.A.G. "Metallic sample preparation for phase transformation analysis." *MethodsX*, 2019: 2348-2366
- [2] ASTM. "Standard Guide for Preparation of Metallographic Specimens." *ASTM*. 2017. <https://www.astm.org/e0003-11r17.html> (accessed August 24, 2024).
- [3] ASTM. "Standard Guide for Quantitative Analysis by Energy-Dispersive Spectroscopy." *ASTM*. 2019. <https://www.astm.org/e1508-12ar19.html> (accessed August 24, 2024).
- [4] ASTM. "Standard Reference Test Method for Making Potentiodynamic Anodic Polarization Measurements." *ASTM*. 2021. <https://www.astm.org/g0005-14r21.html> (accessed January 16, 2024).
- [5] ASTM. "Standard Test Methods for Vickers Hardness and Knoop Hardness of Metallic Materials." *ASTM*. 2023. <https://www.astm.org/e0092-17.html> (accessed July 5, 2024).
- [6] Bogdan, Huzum, and Puha Bogdan. "Biocompatibility assessment of biomaterials used in

- orthopedic devices: An overview (Review)." *Experimental and Therapeutic Medicine*, 2021.
- [7] Iuri, S. Brandt, I. Levartoski de Araujo Clodoaldo, Stenger Vagner, G. Delatorre Rafael, and A. Pasa Andre. "Electrical Characterization of Cu/Cu₂O Electrodeposited Contacts." *ECS Transactions*, 2008: 413.
- [8] Matweb. *Matweb*. n.d. matweb.com (accessed August 20, 2024).
- [9] Mohammed, Mohsin Talib, Zahid A. Khan, and Arshad N. Siddiquee. "Beta Titanium Alloys: The Lowest Elastic Modulus for Biomedical Applications: A Review." *International Journal of Chemical, Nuclear, Metallurgical and Materials Engineering* 8, no. 8 (2014): 726-729.
- [10] National Library of Medicine. *Melting Point in the Periodic Table of Elements*. 2023. <https://pubchem.ncbi.nlm.nih.gov/ptable/melting-point/> (accessed August 4, 2024).
- [11] Omazaki. *Arc Flash: Definisi, Bahaya dan Resikonya*. 2023. <https://www.omazaki.co.id/arc-flash-definisi-bahaya-dan-resikonya/> (accessed June 8, 2024).
- [12] R, R Boyer. "Titanium and Its Alloys: Metallurgy, Heat Treatment and Alloy Characteristics." In *Encyclopedia of Aerospace Engineering*, 3-5. Seattle: John Wiley & Sons, Ltd., 2010.
- [13] Reddi, Alluru S. "Intravenous Fluids: Composition and Indications." In *Fluid, Electrolyte and Acid-base Disorders*, by Alluru S. Reddi, 39-54. Springer, 2023.
- [14] Y, Li, Yang C, and Zhao H. "New Developments of Ti-Based Alloys for Biomedical Applications." *Materials*, 2014: 1709-1800.

HALAMAN INI SENGAJA DIKOSONGKAN